PERFORMANCE ANALYSIS OF MULTI-TURN EXTRACTION FROM THE PROTON SYNCHROTRON TO THE SUPER PROTON SYNCHROTRON

Sam Abernethy[1]

[1] *Department of Physics, Engineering Physics and Astronomy, 64 Bader Lane, Queen's University, Kingston, Canada*

Within CERN's accelerator complex, the extraction from the Proton Synchrotron to the Super Proton Synchrotron has been done using the so-called "Continuous Transfer" (CT) method since the 1970's. A new technique, known as Multi-Turn Extraction (MTE), has now been implemented and is in full operation. This report examines a holistic performance analysis of the novel technique in multiple aspects of the accelerator complex, as well as a direct comparison with its predecessor, CT, from the implementation of MTE in 2010 until the end of 2015.

I. INTRODUCTION

The main purpose of this report, and my project over the summer, was to construct a framework with which to conduct a performance analysis of Multi-Turn Extraction (MTE). In Section I A, I will lay out a very brief introduction to the extraction from the Proton Synchrotron (PS) to the Super Proton Synchrotron (SPS), as well as discuss the details of MTE. In Section I B, the figures of merit needed to conduct a performance analysis are defined and discussed. In Section II, the full performance analysis will be conducted, before drawing conclusions and examining future investigations in Section III.

A. Extraction from PS to SPS

The method of beam extraction from the PS to the SPS that had been in use since the 1970's, Continuous Transfer (CT) was based on beam slicing in the horizontal plane with an electrostatic septum. By setting the tune to 6.25, the beam rotated by 90° in phase space after each revolution in the PS. Using this technique, the beam could be extracted over five turns, and sent to the SPS, via the Transfer Lines (TL). Since the SPS is 11 times as long as the PS, this five turn extraction filled $\frac{5}{11}$ of the SPS, meaning that two full extractions were needed to "fill" the SPS, while leaving some space for logistical reasons. This is shown visually in Fig. 1 [1].

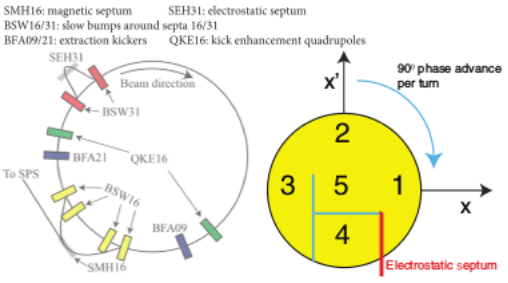

FIG. 1: Basic model of CT extraction.

The main drawbacks of CT were that it caused high radiation levels in the PS, as well as an inconsistent phase shape in the extracted beam. As a result, a novel technique was proposed in 2002: Multi-Turn Extraction (MTE).

MTE is based on an adiabatic crossing of resonance excited by sextupoles and octupoles, in which particles are trapped in stable islands of low-order 1D resonances of horizontal phase space. In less technical terms, the beam is split (via time-evolving magnetic fields) into a "core" and four outer islands. Fig. 2 offers a visual representation of the trajectories of the islands [1].

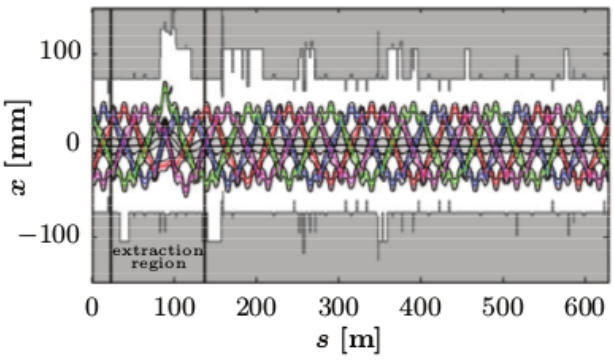

FIG. 2: Evolution of the beam over time; each color represents one of the four outer islands, while the core travels along the center, shown in black.

After being proposed in 2002, it wasn't until 2010 that the first extraction was completed using MTE. At that time, there were large fluctuations in the efficiency over time. After a prolonged effort by many involved with the CERN Beams Department, this fluctuation was tracked down to be caused by a 5 kHz modulation and was largely reduced. As a result of this, MTE officially replaced CT in September 2015 and has been used to extract beam from the PS to the SPS since then.

B. Figures of Merit

The natural figure of merit for MTE is "MTE efficiency," or η_{MTE}. Based on the four outer islands and the core having different intensities, it is a measure of what fraction of the beam is trapped in the outer islands:

$$\eta_{\mathrm{MTE}} = \frac{\langle I_{\mathrm{Islands}} \rangle}{I_{\mathrm{Total}}} \tag{1}$$

In this equation, $\langle I_{\mathrm{Islands}} \rangle$ and I_{Total} stand for the average intensity in the islands and the total beam intensity, respectively. The nominal MTE efficiency is 0.2, which corresponds to equal intensities in the islands and the core.

Another figure of merit is η_{DC}, which can be interpreted as a measure of variability between island intensities (assuming no underlying structural symmetry):

$$\eta_{\mathrm{DC}} = \frac{1}{T} \frac{\left[\int_0^T I(t)\,dt\right]^2}{\int_0^T I^2(t)\,dt} \tag{2}$$

II. PERFORMANCE ANALYSIS

The quantitative analysis of the novel MTE technique is performed by considering the PS and SPS rings, first as separate entities, and then by looking for correlations between the two machines. This is imposed by the present state of MTE, in which fluctuations of the beam parameters are still present, although at a reduced level with respect to the initial beam commissioning. Then, a direct comparison between CT and MTE is carried out to assess the improvements already achieved and the areas still requiring further attention.

For the performance analysis, certain time frames were chosen to analyze from 2010 (for initial MTE operational implementation) as well as 2015 [1] runs. For 2015, one time frame was chosen as representative of the CT extraction technique on September 19$^{\mathrm{th}}$, which was near the end of CT usage. For the MTE data in 2015, the intensity N_p was tested in three separate time frames to probe the following values: 1500, 1800, and 2000, all in 10^{10} ppp. Note that while the first value had been in operation for few weeks, the intermediate one was used for SPS filling only for some hours, on the move towards $N_p = 2000 \times 10^{10}$ ppp, which was the interesting value kept until the end of the 2015 run. The overall picture is shown in Fig. 3, where the PS beam intensity and the extraction efficiency are plotted as a function of time.

To carry out the full performance analysis, certain cuts had to be made on the beam intensity entering the PS and SPS, so as to remove data that was anomalous and varied too widely from the configuration to which the machines were calibrated. In Fig. 3, the raw data for PS intensity is shown before any selection is made, along with the implemented cuts in intensity and corresponding η_{MTE} over time. The cuts used for all time frames are also summarized in Table I.

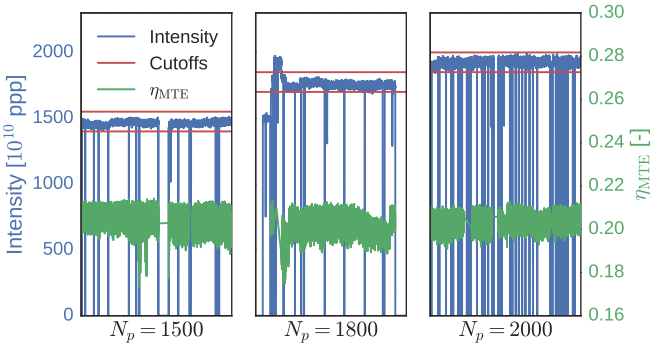

FIG. 3: PS intensity over time, shown together with the cuts in intensity, and η_{MTE}.

	Nominal Intensity	PS Cutoff	SPS Cutoff	Removed data [%]
MTE	1500	< 1400 or > 1600	< 2600	11.1
	1800	< 1700 or > 1900	< 3050	30.2
	2000	< 1850 or > 2050	< 3400	19.3
CT	1600	< 1500 or > 1700	< 2850	10.4

TABLE I: Intensity selection ranges (all units, unless otherwise specified, are 10^{10} ppp). The large percentage of data removed from the sample corresponding to $N_p = 1800$ is due to the period near the start in which the intensity was too high.

A. Proton Synchrotron

The analysis of the PS performance is based on three main figures of merit, namely $\eta_{\mathrm{MTE}}, \eta_{\mathrm{DC}}$ and η_{Ext}. The first two have been already defined, while the last one is PS extraction efficiency. This is obtained by comparing the intensity prior to extraction, as measured by a current transformer in the PS, to the measurement from a current transformer at the beginning of the transfer line.

To evaluate η_{MTE} and η_{DC}, the extracted beam intensity $I(t)$ (also called spill in the following) must be examined. The spill can be acquired by either a low- or a high-sampling rate device. Given the large amount of data generated by the latter, the data used for the analysis reported in this paper is based on the low-sampling rate device. However, for a specific data sample a detailed comparison of η_{MTE} and η_{DC} provided by the two devices has been carried out and a very good correlation was found (featuring a correlation factor ρ around 0.99).

An example of a typical spill for both CT and MTE

can be seen overlaid on top of each other in Fig. 4. These spills have been calculated by restoring the baseline linearity, which is distorted by the electrical properties of the circuits, and by suppressing the resulting constant baseline [2]. It is important to note that the main difference between the two techniques is that the slope of the spill, both at the start and end of extraction, is much steeper for MTE, due to faster kicker rise time in comparison with the CT fast dipoles.

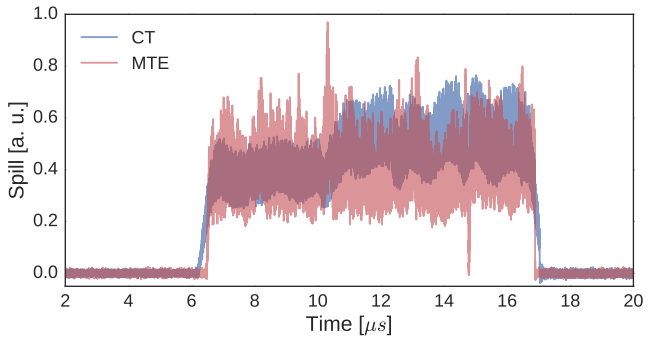

FIG. 4: Example spill for both CT and MTE.

A histogram of η_{MTE} can be seen in Fig. 5. By comparing the 2010 data to 2015, it is clear that there has been a marked improvement in η_{MTE}, which indicates that the sharing between the beam trapped in the islands and that left in the core has been pushed towards the nominal value of η_{MTE}, i.e., ≈ 0.2. Similarly, η_{DC} can be calculated for MTE and CT, and this is shown in Fig. 5. η_{DC} has also increased significantly from 2010 with the MTE technique, at the same time reducing the overall spread, which is a clear indication that the spill shape is flatter and closer to the ideal situation of a constant intensity during the five turns of the extraction.

In terms of PS extraction efficiency, it is worth mentioning that this figure of merit depends on the calibration used to standardize the two devices used to measure the intensity in the PS and in the transfer line. The approach used to determine the calibration of the beam current transformer in the transfer line has been much improved over the years [3], thus making it difficult to compare the results obtained in 2010 with those of the recent 2015 run. An indication of the potential issues with the cross-calibration of the PS and transfer line transformers is given by the presence of values of $\eta_{\mathrm{Ext}} \geq 100$ %, which are clearly non-physical. This situation is not present in the 2015 data, while for the 2010 sample η_{Ext} goes up to 101.2%. As a result, the offset in the calibration procedure was determined to be incorrect and it has been shifted (by 2% in the calculated PS extraction efficiency) so as have the maximum PS extraction efficiency below 100 %. A histogram of η_{Ext} after this offset correction was performed, can be seen in Fig. 6 (upper part). The improvement in terms of extraction efficiency in 2015 over

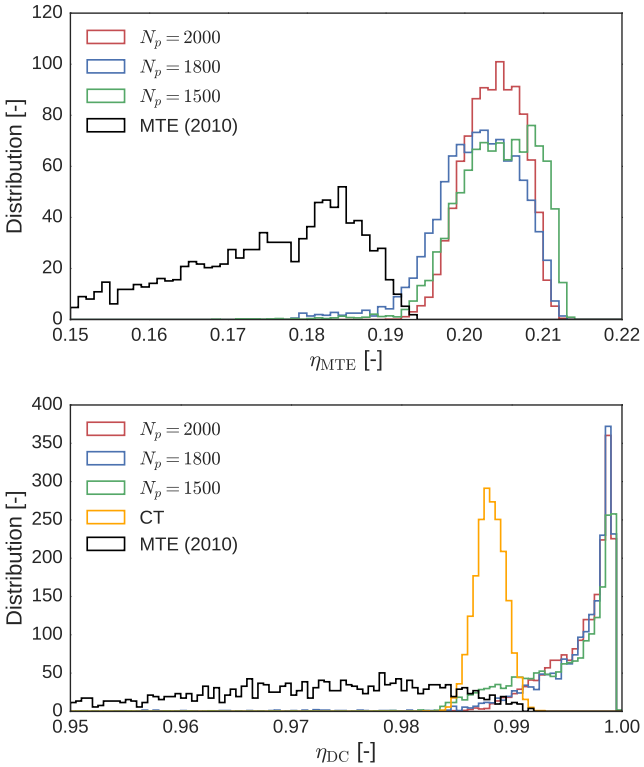

FIG. 5: Upper: Histogram showing the distribution of the MTE efficiency. Lower: Histogram showing the distribution of the DC efficiency from 2010 until 2015, including CT data.

2010 is clearly visible, not only in terms of a higher value of the average η_{Ext}, but also in terms of the shape and population of the tail towards low values of the extraction efficiency, which is much reduced for the 2015 data sample.

Similarly, an efficiency for the transfer line has been defined using as boundaries the first current transformer out of the PS ring, i.e., the same device used for η_{Ext}, and the last device before the injection point into the SPS. The distribution of this figure of merit is also shown in Fig. 6. Data for the 2010 run wasn't taken, thus preventing a direct comparison between the two runs. Nonetheless, the distributions are nicely peaked, without tails, indicating that the fluctuations in η_{MTE} are not affecting the performance of the beam transfer between the two rings (see later).

The last observation, already made in [1], is that only a very mild dependence on the beam intensity is found in the 2015 data, which is certainly an important point for future developments with higher intensity beams. The positive trend in the key figures of merit since the first MTE implementation in 2010, can be seen in Fig. 7.

The key figures of merit $\eta_{\mathrm{MTE}}, \eta_{\mathrm{DC}}, \eta_{\mathrm{Overall}}$ (see next section for the definition of η_{Overall}) are shown for the 2010 and 2015 MTE runs. For the 2015 case, the beam

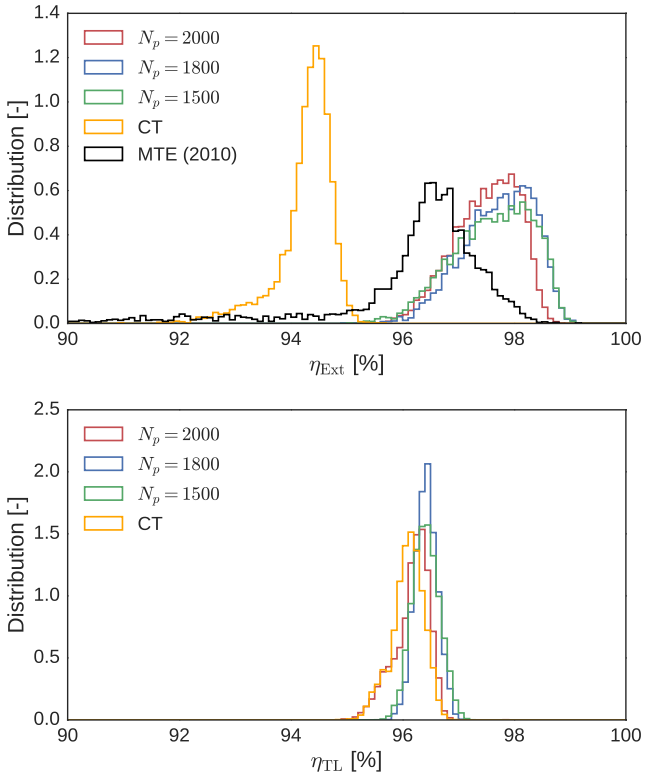

FIG. 6: Upper: Histogram showing the distribution of the PS extraction efficiency. Lower: Histogram showing the distribution of the transfer line transmission efficiency.

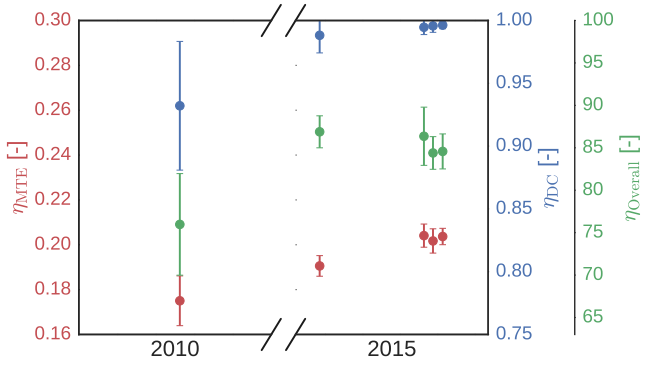

FIG. 7: MTE figures of merit over time ($\eta_{\mathrm{MTE}}, \eta_{\mathrm{DC}}, \eta_{\mathrm{Overall}}$, see next section for the definition of η_{Overall}). For all three figures of merit shown here there is an improvement from 2010 to 2015 in their values as well as a reduction in the standard deviation (corresponding to the size of the error bars), indicating an increased reproducibility.

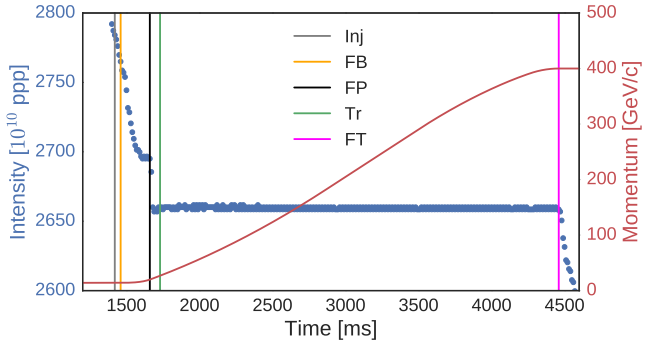

FIG. 8: Example of beam intensity in the SPS as a function of time. Key times shown are Inj, FB, FP, Tr, and FT.

performance at the beginning of the MTE run, which started late in September, as well as during the three time frames with increasing intensity are shown. The improvement of η_{MTE} with respect to 2010 and also in 2015 with respect to the beginning of the run is clearly visible.

B. Super Proton Synchrotron

The standard approach used to qualify the SPS performance is based on the definition of key times along the magnetic cycle at which the transmission efficiencies are examined. The names for these times (and their abbreviations) are as follows: Injection (Inj), Flat Bottom (FB), Front Porch (FP), Transition (Tr), and Flat Top (FT). These times can be seen in Fig. 8 where the evolution of the beam intensity and momentum is shown as a function of time. Note also that transmission efficiencies within the SPS are defined in terms of the transmission from the previous stage to the stage named. As an example, η_{Tr} is defined as the percentage of intensity at FP that gets transmitted to Tr.

It is worth stressing that two extractions from the PS are injected into the SPS, separated by 1.2 s (the PS cycle length for accelerating protons to 14 GeV/c). The SPS Injection Efficiency is the sum of the injected intensities of the two beams from the transfer line, divided by the sum of the two beams' intensities in the transfer line just upstream of the injection point in the SPS.

The distribution of the efficiencies at the various key times are reported in Fig. 9 for the three intensity values used in 2015, including also comparative data from the CT. Wherever possible, the data from the 2010 MTE run is included in the analysis. Similarly to what was observed in the PS, a sizeable improvement is visible both in terms of mean and rms values of the distribution of the efficiency figures compared to 2010. The other important aspect is that the SPS performance clearly depends on the beam intensity, unlike in the PS in which no or only mild dependence on beam intensity was observed.

A metric for the overall SPS performance is given by

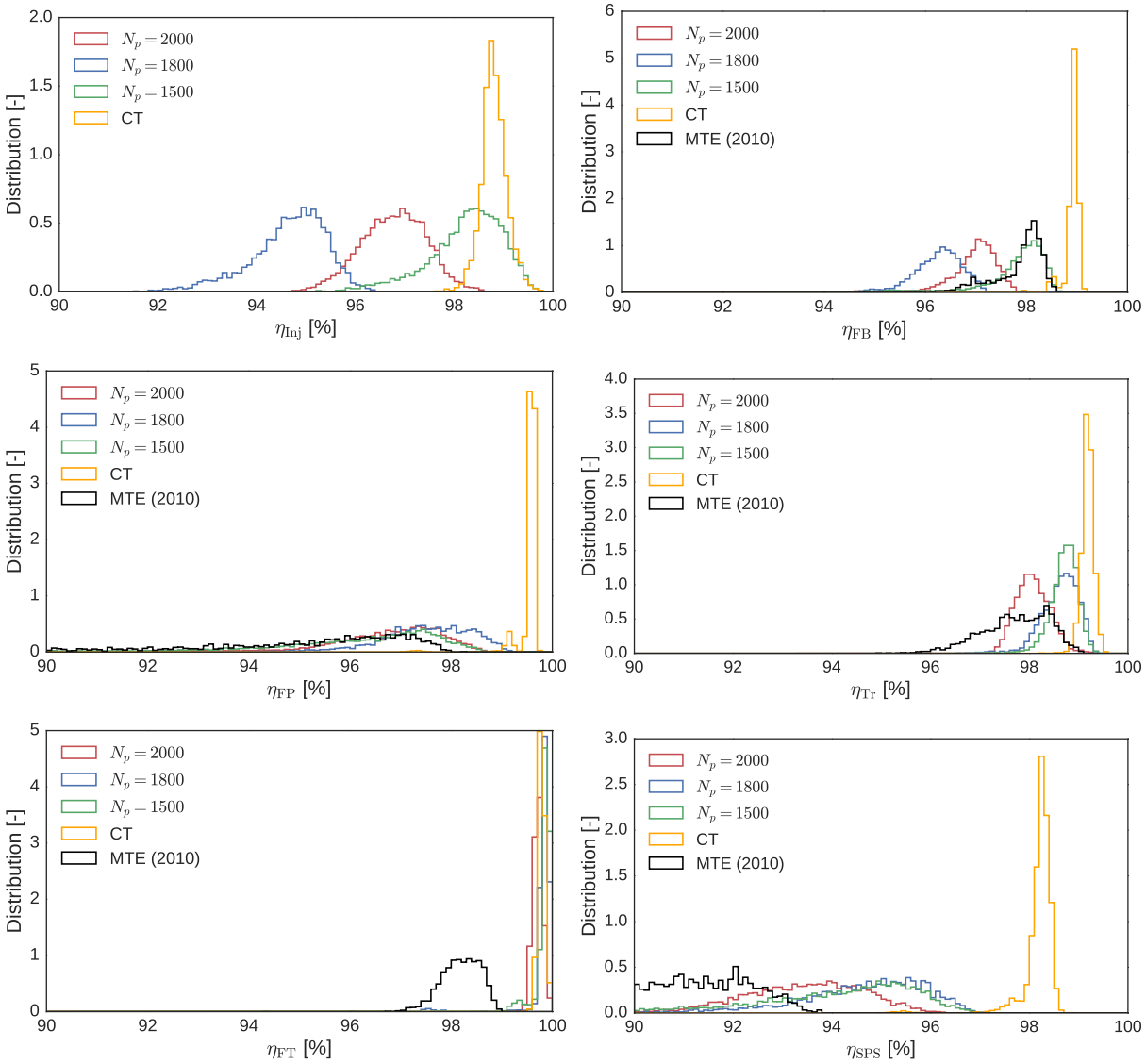

FIG. 9: Global picture of the distribution of the beam transmission through the SPS cycle at key times.

the SPS transmission efficiency, η_{SPS}, defined in terms of the intensity at the end of the SPS cycle (at FT) divided by the sum of the two beams' intensities before ejection in the PS. The histogram is shown in Fig. 9 (lower right plot), where the overall improvement of the transmission efficiency over time is clearly visible and, as expected, features a dependence on beam intensity. η_{SPS} is not the unique indicator of global performance for the MTE beam as one can also include the PS, providing a figure of merit for the efficiency between PS injection and SPS at FT. This indicator is called η_{Overall} and its distribution is shown in Fig. 10. Once more, the MTE improvement over the years is clearly seen as well as a certain dependence on the beam intensity.

The last point to consider is that the previous efficiency indicators, which reflect a time dependence of the losses, can provide insight into the losses distribution as a function of beam momentum. This aspect is essential when evaluating the overall performance of MTE beams, i.e., looking at both machines, PS and SPS, and not focusing on a single one. Indeed, higher-energy particles produce different effects in terms of irradiation and activation, which makes the momentum distribution of beam losses an essential figure of merit. The situation is summarised in Fig. 11. After a full analysis of the intensity losses as a function of momentum, the most significant contribution to the lost intensity comes around 22 GeV/c, corresponding to transition crossing, and the second significant contribution occurs at injection energy. In the other parts of the SPS cycle the losses are negligible.

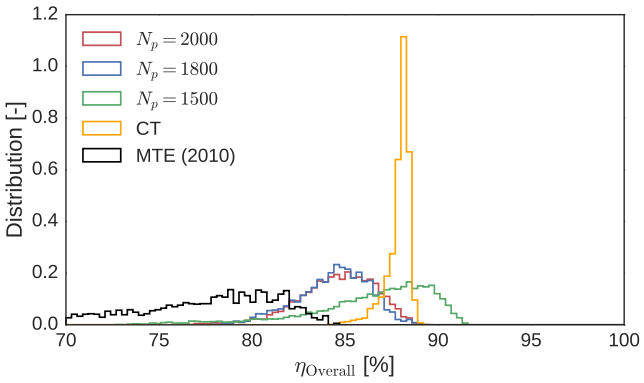

FIG. 10: Histogram showing the distribution of η_{Overall}.

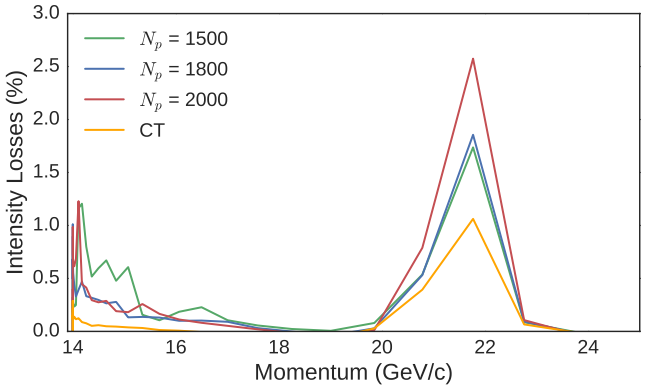

FIG. 11: Intensity losses in % as a function of momentum for 2015 data, both CT and MTE. The highest intensity losses (for all four time frames) come around 22 GeV/c, corresponding to transition crossing, reaching as high as 2.5%.

C. Correlations between PS and SPS

The presence of time variations in the main PS beam parameters like η_{MTE} induces variations in SPS performance. Therefore, a statistical analysis of the correlation between the key efficiencies of the two machines is needed to assess which parameter has the greatest effect on the overall performance.

It is worth noting that whenever the PS and SPS data are to be considered globally, the two PS cycles, which are injected in the same SPS cycle, should in some sense be combined together. For example, the analysis of the correlation of η_{MTE} for two PS consecutive cycles shows a very strong correlation (higher than 0.80) for all data sets examined. This means that the time variations are on a longer time scale than that of the duration of the pairs of 14 GeV/c PS cycles. For this reason, the efficiency indicators of PS cycles injected into the same SPS cycle have been averaged for use in the analysis presented. Furthermore, all SPS cycles in which a single injection from the PS was performed have been rejected and are not part of the data sample discussed.

The correlation analysis outcome is summarised in Fig. 12, where the elements of the correlation matrix are shown as heatmaps. Given the intrinsic symmetries, only the lower-diagonal part of the matrix is shown.

The first conclusion one can draw from the plots is that the overall pattern does not depend strongly on beam intensity. The second immediate conclusion from these heat maps is that there is a rather strong correlation between η_{MTE} and η_{Ext} for all three MTE time frames, which represents a correlation between figure of merits in the same ring. The third conclusion is that the correlations between η_{MTE} and SPS efficiency figures are not very strong. This is an important outcome of the analysis, i.e., that the shape of the spill does not seem to be the main culprit for the SPS performance. In fact, η_{MTE} is positively correlated with losses earlier in the transmission through the SPS cycle (such as η_{TL}, η_{Inj}), but less correlated with later transmission efficiencies. Furthermore, the stronger correlation is only between η_{Ext} and η_{Inj}, suggesting that improving the PS extraction will lead to more effective injection into the SPS. Note that η_{Inj} is less strongly correlated with η_{MTE} thus indicating that a flat spill is less important, as far as SPS injection losses are concerned, than a clean PS extraction. It is also worth mentioning that most of the correlations are positive, indicating that an improvement in the PS would also be beneficial for the SPS.

To examine this further, the correlation plots for some of the SPS efficiencies against η_{MTE} are shown in Fig. 13. The progressive reduction of the correlation of SPS figures of merit and η_{MTE} is clearly visible as well as a non-negligible number of outliers: in spite of their impact on the numerical value of the correlation, which could be higher if we rejected outliers, the plots clearly indicate that the reduction of correlation is real.

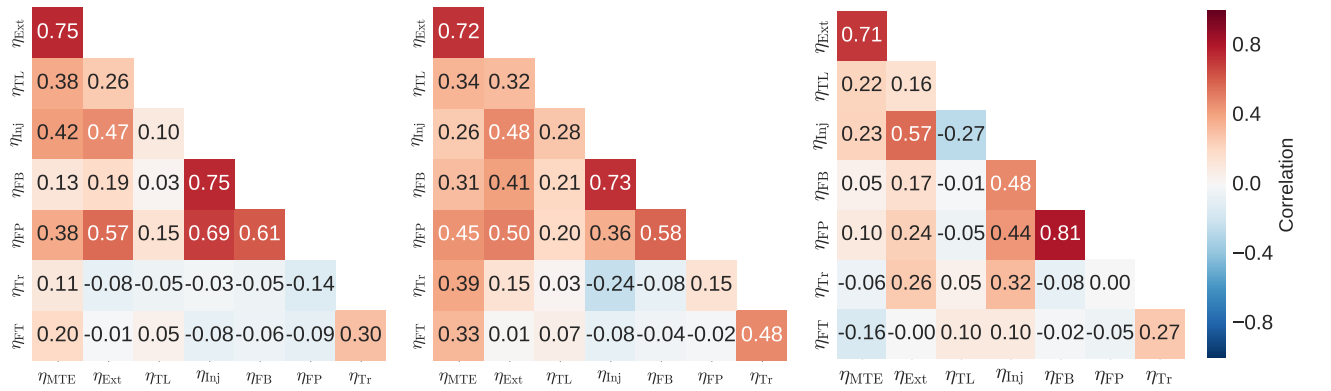

FIG. 12: Correlation heat maps for the figures of merit used in the analysis. The three plots refer to the different MTE beam intensities, namely $N_p = 1500, 1800, 2000$ ppp for the left, centre, and right panel, respectively. It is worth noting the general tendency of correlations to be positive.

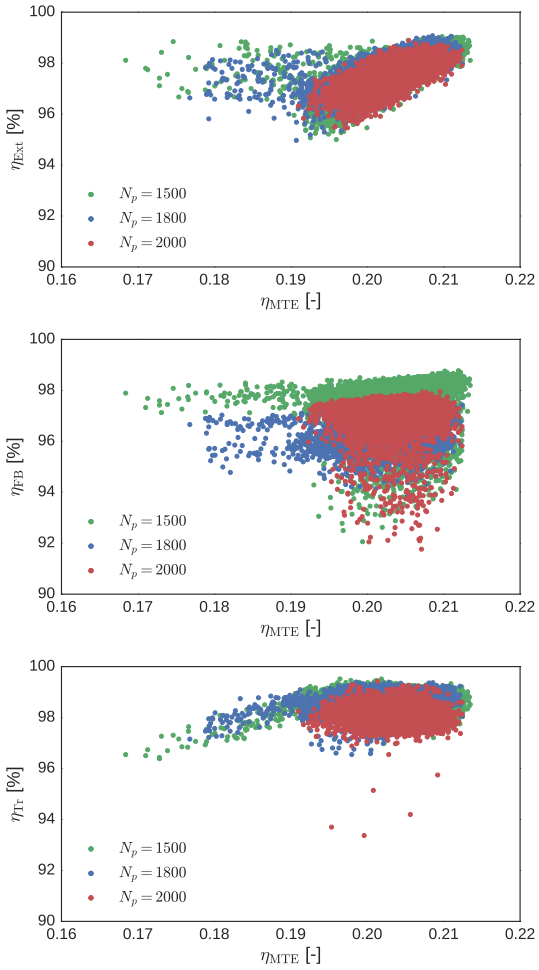

FIG. 13: Example of correlation plots between PS and SPS efficiency figures of merit. The progressively lower correlation between η_{MTE} and transmission efficiencies for later stages in the SPS cycle is clearly visible.

D. Comparison between CT and MTE beams

The last point that will be addressed is the direct comparison between CT and MTE. The key quantities have been already shown in previous plots and in this section the main points will be presented. At the level of the PS ring, the MTE features a flatter spill than CT as can be seen in Fig. 5, where the distribution of η_{DC} is shown. In fact, even though MTE features longer tails in the distribution of η_{DC}, the minimum value is still comparable with that of CT and the peak is much closer to 1. Moreover, MTE is also superior in terms of η_{Ext} (see Fig. 6). The transfer line efficiency η_{TL} features very similar distributions for CT and MTE.

As far as the SPS ring is concerned, the situation is somewhat different. The overview of the figures of merit reported in Fig. 9 is rather clear: in general, CT performs better than MTE, with narrower distributions, shifted towards higher values of efficiencies. The differences are particularly striking in the low-energy part of the SPS magnetic cycle, while they are reduced at higher energies and after transition no notable differences are found. As a result, η_{SPS} is rather different (see Fig. 9, lower right) for CT and MTE, mainly due to the differences in the low-energy regime of the SPS cycle. A somewhat different situation is found considering η_{Overall}, where the main difference between CT and MTE is the spread of the distributions, while the mean values are comparable. The losses vs. beam momentum shown in Fig. 11 confirms what was already mentioned, i.e., that in the SPS the losses for MTE are larger than for CT up to around transition and then the differences are no longer relevant.

In terms of correlation between PS and SPS performance, it is interesting to compare the heat maps for MTE, as seen in Fig. 12, and the corresponding situation for CT, as seen in Fig. 14.

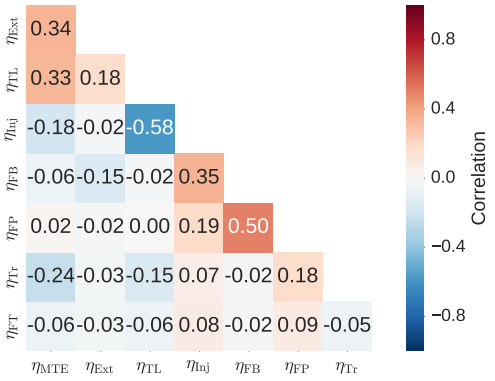

FIG. 14: Correlation heatmap for the figures of merit used in the analysis of CT performance.

The difference between MTE and CT is remarkable: while some correlation can be found for MTE, with CT all correlations are rather weak, as the largest ones are of the order of 0.5 in absolute value. This could be partly due to the smaller fluctuations in the efficiency figures of merit for CT than for MTE (see, e.g., Fig. 9).

As a last point, another way of directly comparing CT and MTE consists of examining the information from the individual beam loss monitors (BLMs) that are installed along both the PS and SPS circumference. For the PS BLMs, Fig. 15 shows the striking improvement of MTE with respect to CT. This is the consequence of the MTE principle, which avoids the beam slicing with an electrostatic septum, leading to a dramatic reduction of beam losses around the PS ring. Note that the plot has been generated using data with $N_p = 1500$ (the closest intensity to that of the CT time frame) and the overall pattern of losses does not differ when other intensities are used. The SPS situation is also visible in Fig. 15. These losses are scaled by the intensity of the beam, so as to give a direct comparison. In most of the BLMs, there are similar levels of losses, but in BLM 121 there is a clear intensity dependence, with an increase of a factor of 2 or more when the highest intensity ($N_p = 2000$) is used.

To summarize the current breakdown of where the losses come from in the PS to SPS extraction mechanism, Fig. 16 shows the losses in each of the four major sections (PS Extraction, Transfer Lines, SPS Injection, and SPS Overall transmission). For the 2010 run, no data is available to evaluate the losses in the transfer line and at SPS injection, so they have been left as 0.0% (to only compare like to like), but the dashed line at the top of the figure shows the overall losses in 2010.

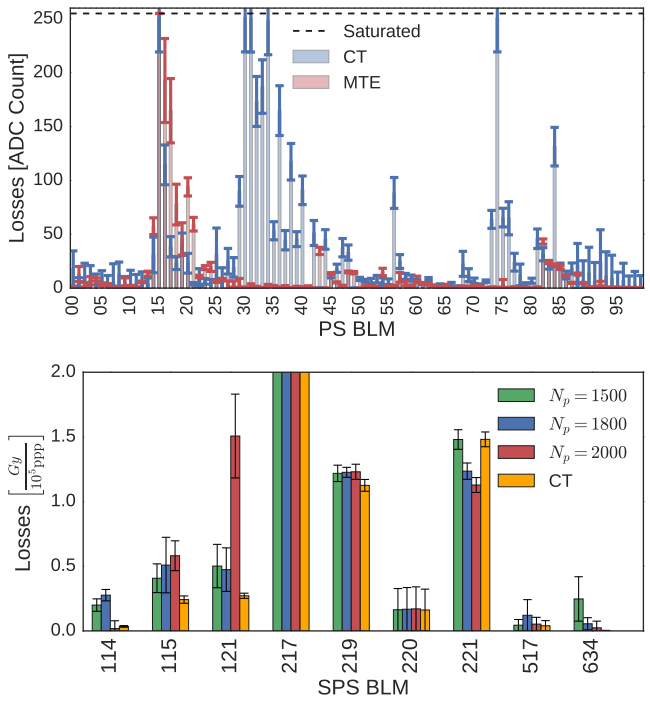

FIG. 15: BLM readings for MTE and CT in the PS (upper) and SPS (lower) rings. For the PS case the readings are given in ADC counts, while for the SPS, the readings have been normalised to the beam intensity.

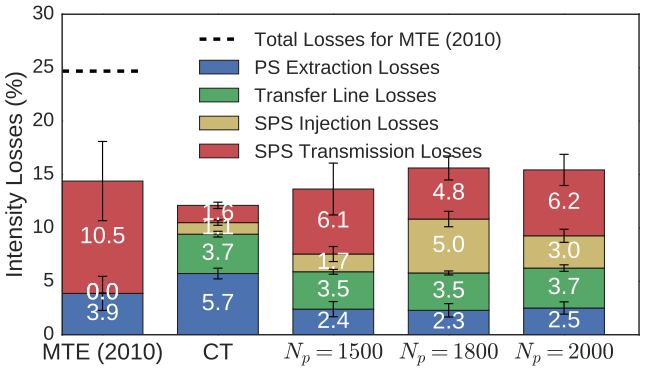

FIG. 16: Bar Plot of Losses for MTE and CT beams. The height of each bar represents the total losses, from before ejection in the PS, to FT in the SPS.

III. CONCLUSIONS AND FUTURE WORK

The first point to note is the huge improvement in MTE global performance since 2010, in all aspects of the accelerator complex. The primary improvement of MTE over CT is found in the PS, where losses have been reduced from 5.7% to roughly 2.4%. The situation in the SPS still favours CT, as far as beam losses are concerned, even while the combined losses in the PS and SPS are almost the same for MTE and CT. It should not be forgotten that CT was implemented in the 1970's, fully optimized over the course of decades, and the level of losses shown in Fig. 16 are the results of long and meticulous work. Clearly, MTE is comparatively very new and still has room for major improvements, but is rapidly increasing efficiency over the years.

Efforts are ongoing in the CERN Beams Department to further improve efficiency, determine correlations between figures of merit, and investigate sources of losses throughout the accelerator complex. This performance analysis framework, constructed to analyze the 2015 data, will continue to be used to examine the 2016 data later this year.

IV. ACKNOWLEDGEMENTS

It is with sincere appreciation that I thank Dr. Massimo Giovannozzi and Dr. Guido Sterbini for their supervision and guidance throughout my summer at CERN. I would also like to thank Dr. Adam Sarty and the Institute of Particle Physics, as well as the CERN Summer Student Programme, for making this fantastic experience possible.

[1] J. Borburgh, S. Damjanovic, S. Gilardoni, M. Giovannozzi, C. Hernalsteens, M. Hourican, A. Huschauer, K. Kahle, G. Le Godec, O. Michels, G. Sterbini, EPL **113** 34001 (2016).

[2] J. Bellemann, private communication (2016).

[3] L. Soby, private communication (2016).